Ab initio molecular dynamics calculations on reactions of molecules with metal surfaces

Nattino, F.

Cover Page

The handle http://hdl.handle.net/1887/35980 holds various files of this Leiden University dissertation

Author: Nattino, Francesco
Title: Ab initio molecular dynamics calculations on reactions of molecules with metal surfaces
Issue Date: 2015-10-28

Chapter 1

General Introduction

1.1 Molecule-Surface Reactions

Molecule-surface reactions are everywhere: They are extensively used in industry [1], where solid catalysts are employed to lower the reaction barriers of chemical processes by detouring the reactants from the direct gas-phase reaction [2]; They are believed to play a major role in the formation of organic molecules and other complex species in star-forming regions in the outer space [3]; They are present in everyday life, in phenomena such as the oxidation of an iron chain, in the catalytic conversion of exhaust gases in automobiles [4], and in the discharge of a battery to obtain electricity [5].

One class of molecule-surface reactions that are of particular interest are reactions on metal surfaces. In heterogeneous catalysis, transition metals are often the active part of the catalyst: they can bind the reactants from the gas-phase, cleave their bonds, provide a good environment for atomic diffusion and formation of new molecules and let the products desorb. Unfortunately, studying the elementary steps that form a catalytic cycle is not a trivial task. The difficulty derives from the fact that the active phase in a real catalyst is usually poorly characterized and inhomogeneously distributed over an inert support with high surface area. Furthermore, catalytic conditions often involve high temperature and pressure.

The complexity of studying gas-surface reactions of catalytic interest can be con-

siderably reduced if a single crystal accurately cut along a particular crystallographic direction and kept under controlled physical conditions is employed as a model for the real catalyst. This approach allows to get some fundamental insight into the elementary steps of the reaction, which is necessary to better understand how a real catalyst works. This knowledge represents the first step towards the ability of improving the catalyst. This approach was used, for instance, by Gerhard Ertl, who was able to propose a reaction mechanism [6] for the ammonia synthesis process, also known as Haber-Bosch process after the industrial chemist who designed it, Fritz Haber, and the chemical engineer who scaled it to industrial level, Carl Bosch. Ertl also suggested that the rate limiting step of this process, which produces ammonia from molecular nitrogen and hydrogen using an iron catalyst, is the N_2 dissociation on the catalyst surface.

Modern surface science instruments allow for preparing, orienting and cleaning crystal samples with very high accuracy. The samples are generally kept at very low pressures (ultrahigh vacuum conditions) to avoid that polluting atoms and molecules would deposit on the surface. A large number of techniques which generally involve the scattering, absorption or emission of electrons, photons and neutrons allows one to characterize surface properties with great detail (see Ref. [7] for an extensive method overview).

In the surface science field, computer simulations have a high potential to help with interpreting experiments: they can provide an atomic-scale movie of a chemical process and they are generally cheaper, safer and faster than regular laboratory experiments. Nowadays, theoretical methods are able to very accurately reproduce experimental observables for gas-phase reactions. The same level of accuracy, however, is far from being achieved for reactions on metal surfaces. This has to do with the large number of electrons present in transition metals, and with the peculiar electronic and mechanical properties arising from the periodic nature of surfaces. In the field of surface science, the accuracy of theory is such that it can generally provide a semi-quantitative description of equilibrium structures, adsorption energies, reaction coordinates and activation energies but further improvement has to be achieved to be able to quantitatively reproduce or predict experimental observables. Note that the accuracy of theoretical methods

can only be tested against experimental data measured under accurately determined conditions, so that they can be modeled as carefully as possible in the simulations.

The adsorption of a molecule on a metal surface often represents the first step in a catalytic cycle. A large number of studies have focused on the reactive and the non-reactive scattering of molecules from surfaces with the aim of improving the fundamental understanding about the adsorption phenomenon. Note that also the study of the molecules that bounce back after the impact with the surface is relevant, since they may carry detailed information about the molecule-surface interaction that they experienced during the collision. In the next section we discuss the adsorption phenomenon together with the other possible outcomes of the collision of a molecule with a metal surface.

1.2 Reactive Scattering of Molecules from Metal Surfaces

In general, the outcome of a molecule-surface collision is determined by the details of the interaction potential between the molecule and the surface. It is important to mention, however, that the molecule does not simply interact with an infinite ideal lattice through a single potential energy surface, but other elements might play a role. First of all, surface atoms might be displaced from their equilibrium positions due to their thermal motion, and this might modify the interaction potential. Furthermore, the impacting molecule can exchange energy with the lattice, due to the coupling with lattice vibrations (phonons). In addition, the continuum of electronic states that characterizes a metal surface enables a second energy exchange channel between the molecule and the surface. Arbitrary small amounts of energy, in fact, can be transferred from the molecular degrees of freedom to the electrons lying just below the Fermi level, generating an electron-hole pair. In order to model the effect of electron-hole pair excitations, multiple electronic states and the couplings between them have to be taken into account. These effects are often called non-adiabatic because they cannot be captured if the system is assumed to move on the instantaneous ground state, as in the adiabatic approximation (see also

Section 2.1 in Chapter 2). The role that surface temperature, surface motion, and non-adiabatic effects play in molecule-surface reactions might differ from system to system.

In discussing the reactive scattering of molecules from metal surfaces we will focus on diatomic molecules for simplicity (Section 1.2.1), but we will also discuss how the same concepts can be generalized to the case of polyatomic molecules, using methane as a working example (Section 1.2.2).

1.2.1   Diatomic Molecules

Let us consider the simplest type of molecule, a diatomic molecule, like H_2, N_2 or CO. Let's assume the Born-Oppenheimer approximation [8] to be valid, so that the nuclei move on the instantaneous electronic ground state. For a molecule in the gas-phase, the solutions of the Schrödinger equation for the nuclei are labelled by three quantum numbers: v, J and m_J.

The first quantum number, v, defines the vibrational state of the molecule. According to quantum mechanics, only certain vibrational energies are allowed. In Figure 1.1A the interaction energy between two atoms in a diatomic molecule is plotted as a function of the vibrational coordinate, i.e. the bond length of the molecule r. The energy curve has a minimum for $r = r_e$, the equilibrium bond length of the molecule, then it increases for both smaller and larger values of r. For larger values of r, the interaction energy approaches the dissociation energy of the molecule D_e. The horizontal lines in Figure 1.1A represent the allowed energy levels, labeled with the quantum number v.

In addition to the vibrational energy, the magnitude of the angular momentum vector $\mathbf{J}$ and its projection on a space-fixed reference axis (usually labelled as z) $\mathbf{J}_z$ are quantized, such that: $|\mathbf{J}| = \hbar\sqrt{J(J+1)}$ and $|\mathbf{J}_z| = \hbar m_J$, where both J and m_J are integer numbers and $-J \leq m_J \leq J$. Under the rigid rotor approximation, the rotational energy of the molecule $E(J) = \frac{\hbar^2}{2\mu r^2}J(J+1)$, where μ is the reduced mass of the molecule, is a function of only the quantum number J. Therefore, for a fixed value of J, the $(2J+1)$ possible m_J states are degenerate. Note that, for homonuclear diatomic molecules, the symmetry requirements of the molecular wave function allow only certain pairings of
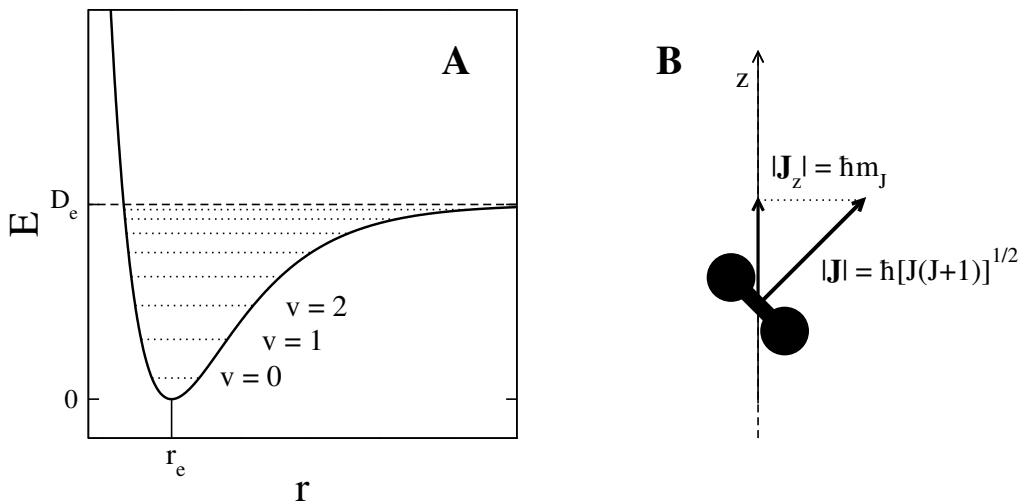
Figure 1.1: (A): Interaction energy as a function of the bond length for a diatomic molecule. The equilibrium bond length and the dissociation energy are labeled as r_e and D_e, respectively. (B): Classical representation of a molecule in the rotational state (J, m_J).

rotational states and nuclear spins. In particular, the molecular wave function has to be either symmetric or antisymmetric with respect to the interchange of the nuclei for nuclei with integer spin (bosons) or half-integer spin (fermions), respectively. The nuclear spin state can be either symmetric (ortho) or antisymmetric (para) with respect to this symmetry operation. The same is true for the rotational part of the molecular wave function, which is symmetric and antisymmetric for even and odd values of J, respectively. The vibrational part of the molecular wave function for a diatomic, on the other hand, is always symmetric. Therefore, the only combinations allowed for nuclear spin states and rotational states are the ones for which these two parts of the molecular wave function have the same symmetry with respect to the nuclei interchange for bosons (e.g. in D_2), while the opposite is true for fermions (e.g. in H_2).

The classical representation of a molecule in a specific (J, m_J) rotational state is depicted in Figure 1.1B. Note that $\mathbf{J}$ is always perpendicular to the bond of the molecule, and that m_J defines the orientation of $\mathbf{J}$ in space. This suggests that there is a correlation between the rotational state of the molecule (J, m_J) and its spatial orientation. More precisely, $|m_J|$ defines the rotational alignment of the molecule with respect to the z-

axis: high $|m_J|$ states correspond to 'helicopter'-like rotation, with the molecular bond close to be perpendicular to the z-axis, while low $|m_J|$ states correspond to 'cartwheel' rotations, with the molecular bond also sampling configurations parallel to the z-axis.

For what concerns the translation of the center of mass of the molecule, the solutions of the nuclear Schrödinger equation represent a continuum of states. Therefore, the translational energy can assume all possible values.

When a molecule in the initial state (v, J, m_J) and linear momentum $\mathbf{k}$ approaches a clean metal surface, a large variety of phenomena can occur. We can divide these phenomena in two broad classes of events: the molecule can bounce back towards the vacuum, in what we call a scattering event, or the molecule can adsorb on the surface.

1.2.1.1   Scattering

Scattering events can be classified according to the final state and momentum vector associated with the molecule when leaving the surface, (v', J', m'_J) and $\mathbf{k}'$, respectively. If $v' = v$, $J' = J$, and $|\mathbf{k}'| = |\mathbf{k}|$ we talk about *elastic scattering*, which means that energy is neither exchanged with the surface nor is it shuffled between the various molecular degrees of freedom. On the other hand, *vibrationally inelastic scattering* and *rotationally inelastic scattering* occur when the interaction with the surface leads to a change of vibrational state $(v' \neq v)$ or rotational state $(J' \neq J)$ of the molecule, respectively. Inelastic scattering can be both a consequence of the strong coupling that the surface interaction potential induces between the internal molecular degrees of freedom or a signature of energy exchange with the surface. Finally, when interacting with the periodic potential of the surface, the molecule can undergo *diffraction*, revealing its dual wave-particle nature. This is a consequence of Bloch's theorem [9, 10], according to which the wave function of a particle in a periodic potential can always be written as a function with the same periodicity of the potential times a phase factor. It can be shown that in such a periodic potential the linear momentum components parallel to the surface can only change by discrete amounts, so that $k'_x = k_x + n\Delta k_x$ and $k'_y = k_y + m\Delta k_y$, with n and m integer numbers. Note that these quantization rules are exactly followed in the
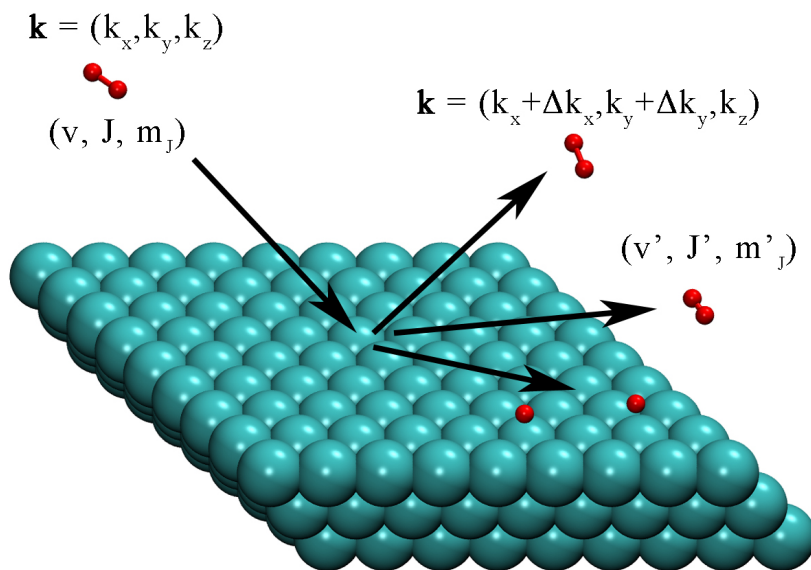
Figure 1.2: Graphical representation of some of the possible outcomes that can follow the approach of a molecule to a metal surface: molecular diffraction, inelastic scattering and dissociative chemisorption, in clockwise order.

limit that no energy transfer to or from the surface occurs, in which case experiments can determine the probabilities for diffractive scattering (possibly accompanied by rotational transitions as well) by measuring the intensity of the molecules scattered to specific solid angles and taking into account the effect of energy conservation. The diffraction quantum $\Delta \mathbf{k}$ is then a surface reciprocal lattice vector, and is therefore determined by the periodicity of the (direct) lattice. The $n = m = 0$ special case of diffraction is often called *specular reflection* or *specular scattering*.

1.2.1.2 Adsorption

We have already mentioned that a gas-phase molecule can adsorb on a metal surface. Different kinds of adsorption exist. According to a first classification, we can divide adsorption into *physisorption* and *chemisorption*. A molecule is physisorbed on a surface when it weakly interacts with the substrate, generally through van der Waals forces. Chemisorption, on the other hand, occurs when the electron density rearranges itself to form new chemical bonds between (parts of) the molecule and the surface. The

chemisorption process can be classified as activated or non-activated: in the first case an energy barrier has to be overcome by the impinging molecules in order to adsorb on the surface, while at least one barrierless adsorption path exists in the second case.

Chemisorption can be either dissociative or molecular, depending on whether one or more bonds in the molecule are broken during the adsorption process. The dissociative chemisorption is a consequence of the interaction between the bonding and anti-bonding electronic states of the gas-phase molecule with the surface valence electrons. In particular, the molecular states are broadened due to the interaction with the surface s and p electrons, while they are split in surface bonding and surface anti-bonding states due to the interaction with the d-states [11, 12]. If both surface bonding and molecular anti-bonding states are populated (i.e. they are below the Fermi level), the molecule can dissociatively chemisorb on the surface.

1.2.2   Polyatomic Molecules: Methane

What we described so far applies to diatomic molecules, but can be generalized to polyatomic molecules, like methane. Within the harmonic oscillator approximation, the normal mode description can be employed for representing the molecular vibrations. A molecule constituted by N atoms, has $3N - 6$ vibrational degrees of freedom ($3N - 5$ if linear), which can be grouped into vibrational modes. Each mode belongs to an irreducible representation of the point group of the molecule. The degeneracy of a vibrational level is given by the number of isoenergetic vibrational states corresponding to this level. Vibrational modes are composed of the collective motion of many atoms in the molecule. As an example, the vibrational modes of methane are illustrated in Figure 1.3. Normal modes generally involve a strong coupling between identical oscillators in the molecule. For instance, both the symmetric (ν_1) and the antisymmetric (ν_3) stretch modes in methane involve the simultaneous stretch of the four (identical) CH bonds of the molecule. For the same reason, in the CHD_3 isotopologue of methane, the CH stretch is decoupled from the stretch of the CD bonds.

With respect to rotation, the magnitude of the angular momentum vector and its
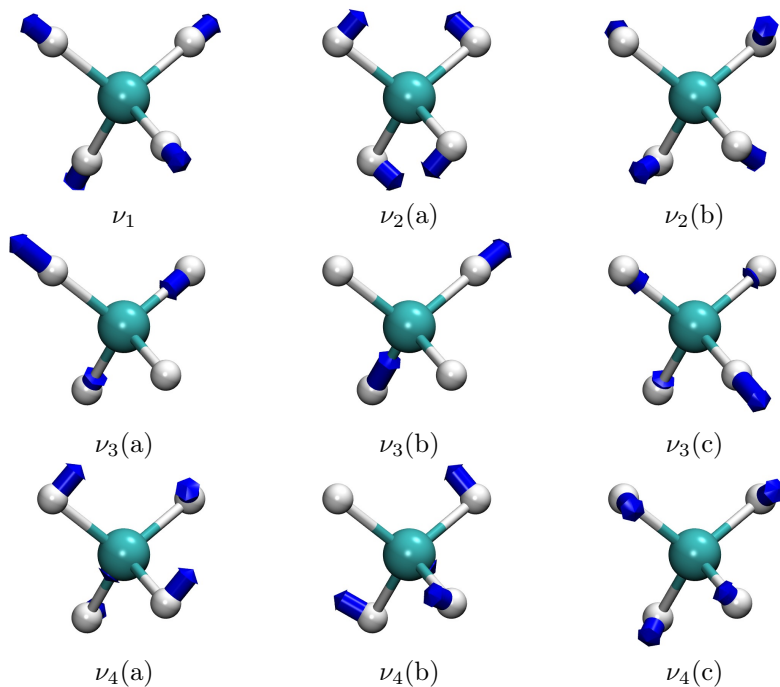
Figure 1.3: Representation of the four vibrational modes of methane (CH_4).

projection on a space-fixed reference axis are quantized for polyatomic molecules as for diatomic molecules, the corresponding quantum numbers being J and M, respectively. In addition, for molecules in which at least two of the three principal inertia moments are equal to each other (symmetric and spherical top rotors), a third quantum number K reflects the quantization of the projection of the angular momentum vector on the principal axis of rotation of the molecule. The quantum number K (as M) can assume integer values in the range $[-J; J]$. In methane, the three principal inertia moments are all equal to each other so that the molecule can be classified as a spherical top rotor. Under the rigid rotor approximation, the rotational energy is $E(J) = \frac{\hbar^2}{2I} J(J+1)$, where I is the inertia moment, as for diatomic molecules. Note that $E(J)$ does not depend on M and K, so that the degeneracy of the J rotational level is $(2J + 1)^2$. CHD_3, on the other hand, is classified as a oblate symmetric top rotor, because the moment of inertia of the rotation about the symmetry axis of the molecule (the so-called 'umbrella' axis), $I_\parallel$, is bigger than the moment of inertia along any of the perpendicular directions

$(I_\perp)$. For a oblate symmetric top, the K degeneracy is lifted and the rotational energy is given by $E(J, K) = \frac{\hbar^2}{2I_\perp} J(J+1) + \left(\frac{\hbar^2}{2I_\parallel} - \frac{\hbar^2}{2I_\perp} \right) K^2$. The degeneracy of the rotational level (J, K) is therefore $(2J + 1)$, since it is only due to the quantum number M. Note that the energy expression for a symmetric top rotor does not depend on the sign of K, therefore the rotational levels (J, K) and $(J, -K)$ are degenerate (for $K = 0$ only one level exists). Note also that for methane, as for diatomics, the symmetry constraints on the total molecular wave function allow only certain pairings of rovibrational states with nuclear spin states.

The same outcomes as for diatomic molecules can be expected for a methane molecule approaching a metal surface: elastic and inelastic scattering, adsorption. Note, however, that for methane the vibrationally inelastic scattering can involve vibrational (de-)excitation (as for diatomic molecules) of a specific mode but also energy transfer from one vibrational mode to another.

1.3   Aim of This Thesis

Many state-of-the-art methods for modeling gas-surface reaction dynamics consist of three steps: first, the molecule-surface ground-state interaction energy is calculated for various molecular configurations through a suitable electronic structure method (usually density functional theory [13,14] at the generalized gradient approximation level [15–18]); next, the computed energy points are fitted or interpolated to obtain a continuous expression of the energy as a function of the molecular configuration (the so-called potential energy surface, PES [8, 19]); finally, dynamics is performed on the pre-calculated PES [20, 21]. The second step sets some limitations to the general applicability of the method just described to the field of molecule-surface reactions. In fact, performing an accurate fitting or interpolation of pre-calculated energy points is a very complex task for a large number of nuclear degrees of freedom (> 6). Therefore, the calculations that employ this approach often involve the static surface approximation (or model surface temperature with approximate methods) [22–30]. For the same reason, untested dynamical approximations or model potentials are necessary for describing the reaction of

polyatomic molecules on surfaces [31–37].

The aim of this thesis has been to apply the *ab initio* molecular dynamics (AIMD) technique to the study of reactions on metal surfaces. This technique is not new [38–40], nor is its application to the field of surface science [41–43], but only recently it became possible to calculate experimental observables (like dissociation probabilities) with reasonable statistical accuracy [44]. The use of AIMD bypasses the need of pre-computing and fitting the PES, since the forces acting on the nuclei are calculated at each time step of the dynamics. By using AIMD we achieved two main goals: first, we were able to model the effects of surface temperature and lattice recoil through the inclusion of surface-atom motion, and to study how these affect two prototypical gas-surface reactions; second, we could model the reaction of a polyatomic molecule on metal surfaces, without the need of introducing *a priori* dynamical approximations for the nuclear motion. The AIMD method is described further in Chapter 2.

1.4   Main Results

Overall, three systems have been the object of study. Chapter 3 and Chapter 4 are about the dissociation of hydrogen on a copper surface. This system is not important because of particular industrial applications but its relevance comes from the large number of experimental and theoretical studies which focused on this molecule-surface reaction, such that it is considered a benchmark for activated dissociative chemisorption. This system is ideal for testing the accuracy of theoretical models and electronic structure methods, since evidence exists that this reaction is, essentially, electronically adiabatic [45]. Previous calculations that used the static surface approximation were able to reproduce with high accuracy several observables that were either measured at low surface temperature or weakly dependent on surface temperature [27, 28]. These calculations, however, failed at reproducing some observables computed at high surface temperature such as the rotational quadrupole alignment parameter [46], which is a parameter that expresses the dependence of the reactivity on the rotational alignment of the molecule. In Chapter 3 we show that surface temperature effects modeled with AIMD on average lower the

alignment parameter for D_2 reacting on Cu(111), considerably improving the agreement between theory and experiments. We also show that the initial state-selected reaction probability is slightly improved against static surface calculations, for the two initial states for which the rotational alignment parameter has been computed.

The initial state-selected reaction probability of D_2 on Cu(111) is the main topic of Chapter 4. Pre-existing discrepancies between static-surface calculations and experimental data have been tackled by running new AIMD calculations modeling surface temperature effects and by performing an improved analysis of the raw experimental data [47]. We have also simulated time-of-flight spectra from theoretical reaction probabilities in order to compare theory to experiments without performing any manipulation of the raw measured data. Results show that the new analysis of the experimental data improves the agreement between theory and experiments: by using more flexible functions to fit the experimental data, we obtain reaction probability curves of which the saturation value does not depend on the initial vibrational state, as found in the simulations, whereas the opposite was suggested by the original analysis of the data. Furthermore, the mean absolute error of the energy at which the initial state-resolved reaction probability equals half the experimental saturation value (the so-called effective barrier height) is now lower than 1 kcal/mol (limit that defines the chemical accuracy) for both static-surface and AIMD calculations. As also found in Chapter 3, only a slight improvement in the initial state-selected reaction probability curves is obtained over the static surface calculations when modeling surface temperature effects with AIMD.

Chapter 5 focuses on methane dissociation on a platinum surface. The dissociation of methane on metals is both of practical and fundamental interest. The cleavage of the CH bond of the molecule and the consecutive adsorption of the methyl fragment and the hydrogen atom on a nickel catalyst is the first and a rate limiting step of the steam reforming process [48], which is the main commercial source of molecular hydrogen. Molecular beam experiments showed that the reactivity depends non-statistically on the way in which energy is disposed in the different degrees of freedom of the molecule [49–51]. In Chapter 5 we present AIMD calculations based on the PBE density functional on the

reactivity of the trideuterated isotopologue of methane CHD_3 on Pt(111). Experiments that used a laser to vibrationally excite the CH stretch mode of the reacting molecules showed that the excitation of this mode significantly enhances the reactivity [52]. Furthermore, CHD_3 molecules which normally dissociate to give $H_{(a)}$ + $CD_{3(a)}$ and $D_{(a)}$ + $CHD_{2(a)}$ with the statistical relative ratio 1:3, only produce $H_{(a)}$ + $CD_{3,(a)}$ upon excitation of the CH stretch mode [52,53]. Our calculations reproduce the experimental branching ratios and semi-quantitatively describe the experimental sticking probability as a function of the average collision energy of the molecules. We have also tested the validity of the dynamical approximations which have been previously used for modeling the methane dissociation reaction [31–35]. We have found that a sudden approximation, which assumes that a degree of freedom can be 'frozen' when it does not change considerably in the dynamics, could be used in the calculation of the reaction probability to describe the lateral motion of the molecule and its rotation. Finally, we have investigated the role played by the surface atom motion in the dynamics, and we have found that the surface atom below the dissociating molecule is on average outside the surface plane for reactive trajectories at low collision energies. This finding is consistent with previous studies according to which the motion of the surface atom towards the impinging molecule lowers the barrier for dissociation [32, 54–56]. These observations can explain the strong surface temperature dependence observed for methane dissociation on metal surfaces [57].

In Chapter 6 we study the effect of the density functional on calculations of methane dissociation on Pt(111). Our goal is to find a semi-empirical density functional able to accurately describe the reactivity of molecular beams in which only a fraction of the molecules is vibrationally excited ('laser-off' molecular beams), and of molecular beams in which the CH-stretch mode has been excited with a laser. Various density functionals are considered, including functionals that account for the van der Waals interaction. This type of functional has recently been shown to work reasonably well for describing the reaction of H_2 [58] and N_2 [59] on metal surfaces. The density functional that returns the overall best agreement with experimental data is a functional consisting

of the correlation functional from Dion et al. [60], developed to mimic van der Waals interactions, and a linear combination of the RPBE and PBE exchange functionals. In particular, this functional produces good agreement with the experimental laser-off data at the lowest collision energies simulated, and with the CH-stretch excited data, thereby improving over the PBE description.

Finally, the dissociation of nitrogen on a tungsten surface (W(110)) is the topic of Chapter 7. This system is relevant as a model system for heterogeneous catalysis, as the N_2 dissociative adsorption on iron is believed to be the rate limiting step of the ammonia synthesis process already mentioned in Section 1.1. In fact, tungsten and iron exhibit some similarities with respect to nitrogen adsorption. For instance, both metals are characterized by a large crystallographic anisotropy, which means that the N_2 adsorption properties highly depend on the crystallographic face of the metal exposed to the molecules [61]. Accurately modeling the reactive and non-reactive scattering of N_2 from tungsten surfaces is a challenge that has not yet been met [25, 59, 62–65]. In Chapter 7 we have investigated the effect of surface atom motion on the reactivity of N_2 on W(110) using AIMD, testing two density functionals for the electronic structure calculations. In particular, we have found that modeling lattice motion in the dynamics strongly increases the reactivity, and we suggest that this has to do with the availability of very deep molecular adsorption wells in the PES and the large energy exchange with the surface, such that molecules remain trapped in the proximity of the surface with a higher chance to react than in the frozen-surface simulations [25, 62, 63].

1.5   Outlook

In the last section of this chapter we discuss the possible research directions that could follow the work described in this thesis and the open questions that require further investigation.

Given the benchmark status of the H_2+Cu system and given the high accuracy that could be achieved in modeling many observables for this system [27, 28], it would be desirable to understand the reason of the disagreement still present between theory

and experiment in the description of the rotational quadrupole alignment parameter $A_0^{(2)}$. Further work should be directed to reduce systematic errors in the AIMD method (e.g. by increasing the surface unit cell size in the model) and to improve the statistical analysis of the experimental data, since the reported measured values of $A_0^{(2)}$ are based on very few measurements (only one data set for one initial rovibrational state). A persisting disagreement between theory and experiment would suggest that the assumption of the validity of detailed balance has to be reconsidered. Other possible sources of errors are inaccuracies in the electronic structure method employed and the neglect of electron-hole pair excitation.

Further work is also desirable to identify the cause of the discrepancy between the theoretical initial state-selected reaction probability curves and the reaction probability curves extracted from desorption experiments [47]. In particular, the dynamical model employed underestimates the surface temperature effect, with theory predicting a smaller broadening of the reaction probability curves with surface temperature than the experiment. Furthermore, discrepancies still exist in the saturation values of the dissociation probability curves. Also for this observable, possible causes of discrepancy include systematic errors in AIMD, the validity of the assumption of detailed balance, and the neglect of electron-hole pair excitation.

An experimental observable that was not accurately described within the static surface approximation [27, 28], and on which the effect of surface temperature has not yet been tested is the probability of vibrational excitation for H_2 scattering from Cu(111) [66]. Modeling this experiment with AIMD might represent a validation test for the ability of this method to describe the effect of phonons on dynamical observables.

Concerning the dissociation of methane on metal surfaces, many points deserve further investigation. We have modeled the dissociation of methane on Pt(111), but the metal that is more relevant to the catalytic steam reforming process is nickel [48]. Preliminary AIMD calculations performed using the PBE exchange-correlation functional (also employed for modeling the dissociation of CHD_3 on Pt(111)) have revealed similar trends for the reactivity on Ni(111) as for Pt(111), and the sticking probability obtained

simulating laser-off molecular beams is too high compared to the experiment [67]. However, the accuracy in modeling molecular beams in which the CH-stretch mode has been excited with a laser for CHD_3 on Ni(111) remains to be investigated. Furthermore, for methane reaction on Ni surfaces, it would be interesting to investigate the use of functionals that account for the van der Waals interaction, as already done for the reaction on a Pt surface.

In the long run, high dimensional quantum dynamics calculations could be used to investigate the role of tunneling in the methane dissociation reaction, but this is best done after identifying a density functional able to produce accurate potential energy surfaces. For what concerns the dissociation of methane on Pt(111), our work suggests that a density functional returning a larger energetic corrugation with respect to the lateral motion of the molecule would improve the overall agreement with the experimental laser-off sticking probability curve. Apart from the sticking probability of CH-stretch excited and laser-off CHD_3 molecular beams, other experimental observables that could be used in tests for the accuracy of a density functional in describing the interaction between methane and metal surfaces are the dependence of the reactivity on the surface temperature [57, 68], the alignment dependence of the reaction [69, 70] and the vibrational mode specificity of the CH_2D_2 [49] and CH_4 [50] isotopologues of methane. Note, however, that the study of the mode specificity for molecules which present vibrational modes the frequencies of which are not sufficiently isolated, might be hampered by the use of classical mechanics, as no constraint avoids that the energy initially disposed into one vibrational mode would flow into other modes within the classical picture.

About the dissociation of N_2 on W(110), the large effect that surface atom motion has on the reactivity at normal incidence, together with the still missing agreement between theory and experiment, raises a number of questions. First of all, the role that surface atom motion might play at high incidence angles is not known. Previous static-surface calculations suggested that the reaction mechanism at high incidence angles can differ from the reaction mechanism at normal incidence [71]. Furthermore, Bocan et al. [63] showed how challenging it is for a density functional to accurately describe this

reaction both at normal incidence and at high incidence angles. Our work suggests that a good functional for this system should predict lower molecular adsorption energies compared to the PBE and RPBE functionals, in order to lower the trapping-mediated reactivity that dominates in AIMD calculations including surface atom motion. It would be interesting to see whether any of the promising van der Waals-corrected density functionals that have been tested by Martin-Gondre et al. [59] for this system within the static surface approximation performs well when modeling surface recoil and surface temperature effects.

In addition to the dissociation probability, another observable for which the effect of surface motion could be investigated is the rotationally inelastic scattering of N_2 from W(110), for which experimental data are available [72]. Moreover, the reactive and non-reactive scattering of N_2 from another tungsten surface, W(100) [73, 74], has not yet been studied with AIMD, simulating the experimental surface temperature. If AIMD calculations, which rely on the Born-Oppenheimer approximation [8], would be able to accurately model both reactive and non-reactive scattering of nitrogen from tungsten surfaces, the importance of modeling electron-hole pair excitation for this system, which is a topic of a recent debate [64, 75, 76], could be ruled out.

Finally, for both the H_2 + Cu system and N_2 + W system the AIMD calculations that we have performed might work as a benchmark for (approximated) methods that aim at modeling surface temperature effects (like the surface corrugation model [77]) and surface recoil effects (like the generalized Langevin oscillator model [78]). These models are attractive since they allow one to compute a large number of trajectories and to propagate them for relatively long times, in such a way that low dissociation probabilities and state-to-state scattering probabilities can be determined with good statistical accuracy.

Bibliography

[1] G. A. Somorjai and Y. Li, Proc. Natl. Acad. Sci. U. S. A. **108**, 917 (2011).

[2] A. Nilsson, L. G. M. Pettersson, and J. K. Nørskov (Eds.), *Chemical Bonding at Surfaces and Interfaces*, Elsevier, Amsterdam, 2008.

[3] R. T. Garrod, S. L. Widicus Weaver, and E. Herbst, Astrophys. J. **682**, 283 (2008).

[4] P. A. J. Bagot, Mater. Sci. Technol. **20**, 679 (2004).

[5] R. Marom, S. F. Amalraj, N. Leifer, D. Jacob, and D. Aurbach, J. Mater. Chem. **21**, 9938 (2011).

[6] G. Ertl, Catal. Rev. Sci. Eng. **21**, 201 (1980).

[7] G. A. Somorjai, *Introduction to Surface Chemistry and Catalysis*, Wiley, New York, 1994.

[8] M. Born and J. R. Oppenheimer, Ann. Physik. **84**, 457 (1927).

[9] F. Bloch, Z. Phys. **52**, 555 (1928).

[10] N. W. Ashcroft and N. D. Mermin, *Solid State Physics*, Saunders College, Philadelphia, 1976.

[11] B. Hammer and J. K. Nørskov, Nature **376**, 238 (1995).

[12] B. Hammer and J. K. Nørskov, Surf. Sci. **343**, 211 (1995).

[13] P. Hohenberg and W. Kohn, Phys. Rev. B **136**, 864 (1964).

[14] W. Kohn and L. J. Sham, Phys. Rev. **140**, A1133 (1965).

[15] J. P. Perdew, J. A. Chevary, S. H. Vosko, K. A. Jackson, M. R. Pederson, D. J. Singh, and C. Fiolhais, Phys. Rev. B **46**, 6671 (1992).

[16] J. P. Perdew, K. Burke, and M. Ernzerhof, Phys. Rev. Lett. **77**, 3865 (1996).

[17] B. Hammer, L. B. Hansen, and J. K. Nørskov, Phys. Rev. B **59**, 7413 (1999).

[18] A. D. Becke, Phys. Rev. A **38**, 3098 (1988).

[19] H. Eyring and M. Polanyi, Z. Phys. Chem. Abt. B **12**, 279 (1931).

[20] M. Karplus, R. N. Porter, and R. D. Sharma, J. Chem. Phys. **43**, 3259 (1965).

[21] R. Kosloff, J. Phys. Chem. **92**, 2087 (1988).

[22] H. F. Busnengo, A. Salin, and W. Dong, J. Chem. Phys. **112**, 7641 (2000).

[23] S. Lorenz, A. Groß, and M. Scheffler, Chem. Phys. Lett. **395**, 210 (2004).

[24] S. Lorenz, M. Scheffler, and A. Groß, Phys. Rev. B **73**, 115431 (2006).

[25] M. Alducin, R. Díez Muiño, H. F. Busnengo, and A. Salin, Phys. Rev. Lett. **97**, 056102 (2006).

[26] J. Behler, S. Lorenz, and K. Reuter, J. Chem. Phys. **127**, 014705 (2007).

[27] C. Díaz, E. Pijper, R. A. Olsen, H. F. Busnengo, D. J. Auerbach, and G. J. Kroes, Science **326**, 832 (2009).

[28] C. Díaz, R. A. Olsen, D. J. Auerbach, and G. J. Kroes, Phys. Chem. Chem. Phys. **12**, 6499 (2010).

[29] I. M. N. Groot, J. C. Juanes-Marcos, C. Díaz, M. F. Somers, R. A. Olsen, and G. J. Kroes, Phys. Chem. Chem. Phys. **12**, 1331 (2010).

[30] I. Goikoetxea, J. Meyer, J. I. Juaristi, M. Alducin, and K. Reuter, Phys. Rev. Lett. **112**, 156101 (2014).

[31] B. Jackson and S. Nave, J. Chem. Phys. **135**, 114701 (2011).

[32] B. Jackson and S. Nave, J. Chem. Phys. **138**, 174705 (2013).

[33] M. Mastromatteo and B. Jackson, J. Chem. Phys. **139**, 194701 (2013).

[34] B. Jiang and H. Guo, J. Phys. Chem. C **117**, 16127 (2013).

[35] B. Jiang, R. Liu, J. Li, D. Xie, M. Yang, and H. Guo, Chem. Sci. **4**, 3249 (2013).

[36] X. J. Shen, A. Lozano, W. Dong, H. F. Busnengo, and X. H. Yan, Phys. Rev. Lett. **112**, 046101 (2014).

[37] P. M. Hundt, B. Jiang, M. E. van Reijzen, H. Guo, and R. D. Beck, Science **344**, 504 (2014).

[38] R. Car and M. Parrinello, Phys. Rev. Lett. **55**, 2471 (1985).

[39] G. Kresse and J. Hafner, Phys. Rev. B **47**, 558 (1993).

[40] G. Kresse and J. Hafner, Phys. Rev. B **49**, 14251 (1994).

[41] A. De Vita, I. Štich, M. J. Gillan, M. C. Payne, and L. J. Clarke, Phys. Rev. Lett. **71**, 1276 (1993).

[42] I. Štich, M. C. Payne, A. De Vita, M. J. Gillan, and L. J. Clarke, Chem. Phys. Lett. **212**, 617 (1993).

[43] I. Štich, A. De Vita, M. C. Payne, M. J. Gillan, and L. J. Clarke, Phys. Rev. B **49**, 8076 (1994).

[44] A. Groß and A. Dianat, Phys. Rev. Lett. **98**, 206107 (2007).

[45] P. Nieto, E. Pijper, D. Barredo, G. Laurent, R. A. Olsen, E. J. Baerends, G. J. Kroes, and D. Farías, Science **312**, 86 (2006).

[46] H. Hou, S. J. Gulding, C. T. Rettner, A. M. Wodtke, and D. J. Auerbach, Science **277**, 80 (1997).

[47] H. A. Michelsen, C. T. Rettner, D. J. Auerbach, and R. N. Zare, J. Chem. Phys. **98**, 8294 (1993).

[48] G. Jones, J. G. Jakobsen, S. S. Shim, J. Kleis, M. P. Andersson, J. Rossmeisl, F. Abild-Pedersen, T. Bligaard, S. Helveg, B. Hinnemann, J. R. Rostrup-Nielsen, I. Chorkendorff, J. Sehested, and J. K. Nørskov, J. Catal. **259**, 147 (2008).

[49] R. D. Beck, P. Maroni, D. C. Papageorgopoulos, T. T. Dang, M. P. Schmid, and T. R. Rizzo, Science **302**, 98 (2003).

[50] R. R. Smith, D. R. Killelea, D. F. DelSesto, and A. L. Utz, Science **304**, 992 (2004).

[51] P. Maroni, D. C. Papageorgopoulos, M. Sacchi, T. T. Dang, R. D. Beck, and T. R. Rizzo, Phys. Rev. Lett. **94**, 246104 (2005).

[52] D. R. Killelea, V. L. Campbell, N. S. Shuman, and A. L. Utz, Science **319**, 790 (2008).

[53] L. Chen, H. Ueta, R. Bisson, and R. D. Beck, Faraday Discuss. **157**, 285 (2012).

[54] S. Nave and B. Jackson, J. Chem. Phys. **127**, 224702 (2007).

[55] S. Nave and B. Jackson, Phys. Rev. Lett. **98**, 173003 (2007).

[56] A. K. Tiwari, S. Nave, and B. Jackson, J. Chem. Phys. **132**, 134702 (2010).

[57] A. C. Luntz and D. S. Bethune, J. Chem. Phys. **90**, 1274 (1989).

[58] M. Wijzenbroek and G. J. Kroes, J. Chem. Phys. **140**, 084702 (2014).

[59] L. Martin-Gondre, J. I. Juaristi, M. Blanco-Rey, R. Díez Muiño, and M. Alducin, J. Chem. Phys. **142**, 074704 (2015).

[60] M. Dion, H. Rydberg, E. Schröder, D. C. Langreth, and B. I. Lundqvist, Phys. Rev. Lett. **92**, 246401 (2004).

[61] S. P. Singh-Boparai, M. Bowker, and D. A. King, Surf. Sci. **53**, 55 (1975).

[62] M. Alducin, R. Díez Muiño, H. F. Busnengo, and A. Salin, J. Chem. Phys. **125**, 144705 (2006).

[63] G. A. Bocan, R. Díez Muiño, M. Alducin, H. F. Busnengo, and A. Salin, J. Chem. Phys. **128**, 154704 (2008).

[64] J. I. Juaristi, M. Alducin, R. Díez Muiño, H. F. Busnengo, and A. Salin, Phys. Rev. Lett. **100**, 116102 (2008).

[65] I. Goikoetxea, J. I. Juaristi, M. Alducin, and R. Díez Muiño, J. Phys.: Condens. Matter **21**, 264007 (2009).

[66] C. T. Rettner, H. A. Michelsen, and D. J. Auerbach, Chem. Phys. **175**, 157 (1993).

[67] E. Dombrowski, E. High, and A. Utz, Unpublished data, 2015.

[68] P. M. Holmblad, J. Wambach, and I. Chorkendorff, J. Chem. Phys. **102**, 8255 (1995).

[69] B. L. Yoder, R. Bisson, and R. D. Beck, Science **329**, 553 (2010).

[70] B. L. Yoder, R. Bisson, P. M. Hundt, and R. D. Beck, J. Chem. Phys. **135**, 224703 (2011).

[71] M. Alducin, R. Díez Muiño, H. F. Busnengo, and A. Salin, Surf. Sci. **601**, 3726 (2007).

[72] T. F. Hanisco and A. C. Kummel, J. Vac. Sci. Technol. A **11**, 1907 (1993).

[73] C. T. Rettner, E. K. Schweizer, H. Stein, and D. J. Auerbach, Phys. Rev. Lett. **61**, 986 (1988).

[74] C. T. Rettner, E. K. Schweizer, and H. Stein, J. Chem. Phys. **93**, 1442 (1990).

[75] A. C. Luntz, I. Makkonen, M. Persson, S. Holloway, D. M. Bird, and M. S. Mizielinski, Phys. Rev. Lett. **102**, 109601 (2009).

[76] J. I. Juaristi, M. Alducin, R. Díez Muiño, H. F. Busnengo, and A. Salin, Phys. Rev. Lett. **102**, 109602 (2009).

[77] M. Wijzenbroek and M. F. Somers, J. Chem. Phys. **137**, 054703 (2012).

[78] H. F. Busnengo, M. A. Di Césare, W. Dong, and A. Salin, Phys. Rev. B **72**, 125411 (2005).